Radial and Axial Compression of Pure Electron

Y. Park, Y. Soga, Y. Mihara, M. Takeda and K. Kamada

Graduate School of Natural Science, Kanazawa University

Kakuma-machi, Kanazawa-shi, Ishikawa 920-1192,Japan

ABSTRACT

Experimental studies are carried out on compression of the density distribution of a pure electron plasma confined in a Malmberg-Penning Trap in Kanazawa University. More than six times increase of the on-axis density is observed under application of an external rotating electric field that couples to low-order Trivelpiece-Gould modes. Axial compression of the density distribution with the axial length of a factor of two is achieved by controlling the confining potential at both ends of the plasma. Substantial increase of the axial kinetic energy is observed during the axial compression.

Keywords

Nonneutral plasma, Rotating Wall, Space-charge-dominated beams

1. Introduction

A pure electron plasma has been expected to use for the investigation of the fundamental properties of space-charge-dominated beam. In principle, the system of a pure electron plasma can reproduce actual situations in high-intensity beam transport channels [1]. Consequently, it is important to understand the accessible density of the electron plasma to simulate the space charge effect of electron beam. In order to control the density of the trapped electron plasma, two methods are usually adopted. One is the rotating wall (RW) technique developed by UCSD group, in which the rotating electric field couples to low-order Trivelpiece-Gould mode [2] or a strong radio-frequency field drives a torque for plasma without tuning to plasma mode [3], as a result plasma density distribution contracts radially. The other is axial compression of the density distribution by controlling the shape of a trap potential.

In this paper we report a preliminary experimental study of the density control of a pure electron plasma by the RW technique and the axial compression in a Malmberg-Penning trap in Kanazawa University. The axial parallel energy distribution of the electron column was estimated as a first step in order to study various features of bunched electron beam.

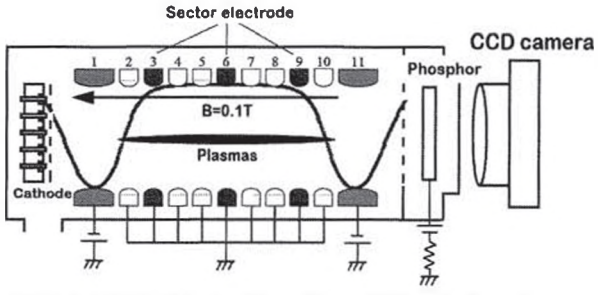

FIG. 1 Schematic configuration of the electron trap.

2. Experimental methods

The schematic configuration of the compression experiments is shown in Fig. 1. The basic scheme of the electron confinement consists of the homogeneous magnetic field B = 0.1 T along the z-axis and the saddle shaped axisymmetric potential with negative barriers at both ends [4]. The electrons are provided from an array of small electron emitters placed in the weaker field zone through the left

barrier, while the confining potential at the plug cylinder is raised to ground in a variable short time. The electrons are disconnected from the sources on the recovery of the potential barrier, the trapped in the cylindrical volume at the center to form a bundle of straight strings with equal length of 170 mm and diameter 1 mm. A radially extended column of electrons is produced by mixing and relaxation of about 500 strings of electrons which accumulate in the trap through multiple injection-hold-mixing cycles. This distribution serves as the initial profile of an electron plasma for the present experimental studies.

Rotating waves are excited in the electron column by applying radio-frequency voltages at variable frequency to the four wall segments azimuthally separated at the axial locations labeled with No. 9 with a phase shift of 90 degrees so as to create a forward-rotating m = 1 mode.

Axial compression is achieved by applying negative voltage to ring electrodes labeled with No.2, 3, 4, 5 and 6 after the confinement, so that a factor of 2 decrease in axial confinement region leads to decrease in the axial length of the eletron plasma.

The measurements of the density profile are made by dumping the whole electrons through the end cylinder on the other side of the cathodes onto a phosphor screen that is biased up to 5 kV from the machine ground. The luminosity distribution on the screen is detected with a charge-coupled-device camera with 512 times 512 pixels and recorded on a computer for numerical analyses. A linear relationship has been confirmed between the total electron number and the luminosity integrated over the screen [5].

3. Experimental Results

3.1 Radial compression analysis

Figure 2 shows time evolution of the two-dimensional density distributions of electrons confined for a period varied up to t = 5 s. The initial density distribution shown in FIG. 2 (a) is axisymmetric and broad. In FIG. 2 (b), with the

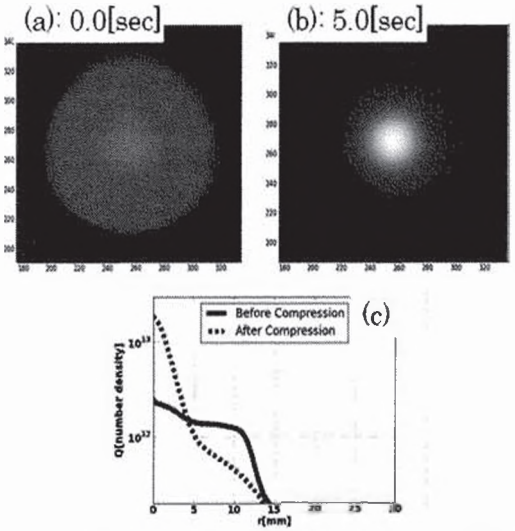

FIG. 2 CCD image describing the density profile of the pure electron plasma in the initial state (a) and after compression (b). (c) Radial distribution of the density profile under the rotating wave. The wall is located at r = 30 mm.

addition of a rotating voltage of the amplitude 2.0 V at the frequency linearly ramped up from 0.1 to 5 MHz for 5 s, the particle distribution contracts radially and the on-axis density is maximized. Figure 2 (c) quantitatively displays the time evolution of the radial density profiles of the images in FIG. 2 (a) and (b). The addition of a rotating field leads to more than 6 times increase of the on-axis density during the period from 0 to 5 sec.

The compression rate (on-axis density normalized by the initial value) under the RW drive depends on various parameters, such as RW amplitude, RW frequency range, and sweep rate of the frequency etc. Time evolutions of the compression rate are compared in FIG.3 (a). Here, the RW drive is carried out during the period from 0 to 0.5 sec under the different frequency range. With the RW drive in broad frequency range from 0.1 to 4 MHz the compression rate reaches 2.8 while the drive with low frequency range from 0.1 to 1 MHz shows no compression. The effective compression occurs in the frequency range from 1 to 2.5 MHz for the initial density distribution. When the RW drive is turned off, the density gradually decays. The maximum compression rate is plotted as a function of the RW

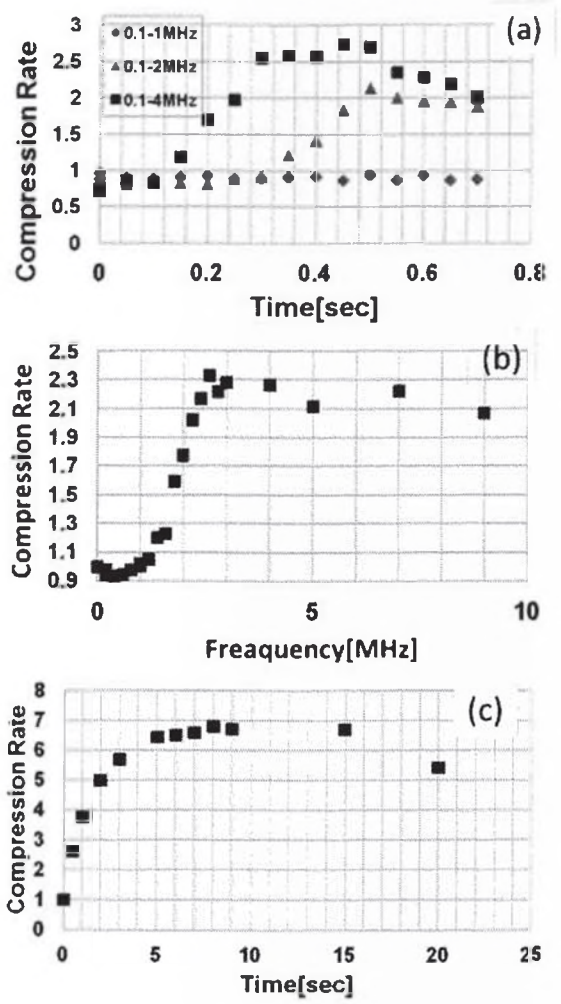

FIG. 3 (a) Time evolution of the compression rate. RW is applied during the period from 0 to 0.5 sec. (b) Compression rate is plotted as a function of stop frequency of RW. (c) Compression rate is plotted as a function of time during RW drive at fixed frequency at 2.8 - 3.0 MHz

stop frequency in FIG. 3 (b). The maximum compression rate rapidly increases in the stop frequency from 1 to 2.5 MHz. Figure 3 (c) shows the maximum compression rate vs. time for RW drive at fixed frequency of 2.8 - 3.0 MHz. For more than 8 s of RW drive the compression rate is nearly constant. The decrease of compression rate for 20 s is due to the outward transport of the particles.

3.2 Axial compression and energy analysis

Next we axially compress the electron plasma right

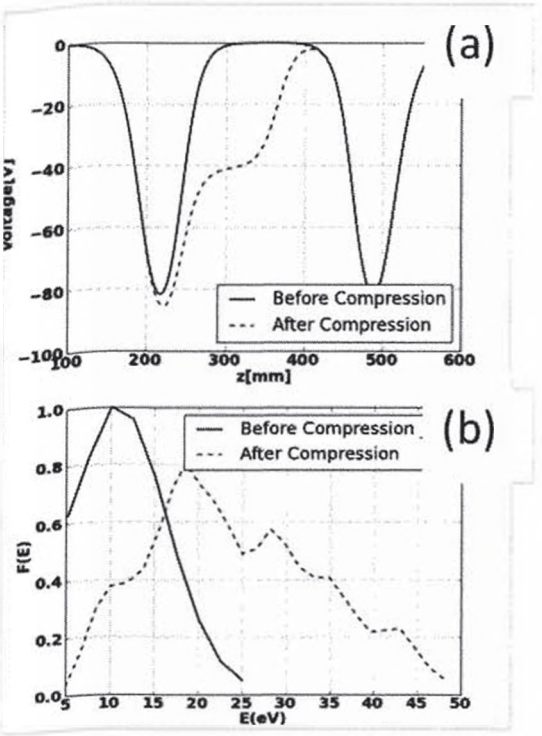

FIG. 4 (a) Axial profile of confining potential on axis for axial compression. (b) Energy distribution function in the initial state (solid line) and after axial compression (dashed line).

after the radial compression with RW drive and measure the parallel energy distribution of the electron plasma. The confinement potential on axis is shown in Fig. 4 (a). Additional negative voltage -42.8 V is applied to the axial region from z = 260 to 330 mm. The method of analyzing the axial kinetic energy of electrons is as follows [6,7]. After the electron plasma is confined for an arbitrary time, the electrons are dumped by a lowered, but non-zero, confinement potential. Electrons with sufficient energy escape from the potential barrier along the magnetic field lines and are collected at a phosphor screen. We measured both the total electron number and the luminosity distribution of phosphor. By repeating the procedure with various barrier potentials, we measured a number of electrons Q_{esc} as a function of the energy E. By differentiating the data, we obtained the parallel energy distribution of the electrons

$$F(E) = \frac{d}{dE}\frac{Q_{esc}}{Q_{all}}.$$

Here Q_{all} is the total electron number. Figure 4 (b) represents the parallel energy distribution function of the plasma. Before compression the distribution has a peak at 10 eV and no particles with the energy more than 30 eV exist. The energy distribution after compression shows a widely expanded distribution from low energy to a high energy of 50 eV. The increase of parallel energy with axial compression may be attributed to an axial acceleration of the particles by rapid change of the confinement potential. Based on the observed axially integrated density and the energy distribution function, we solve the Poisson equation to determine the plasma length. In the result the plasma is compressed with the length from 170 to 80 mm, the density 4.3×10^{13} /m^3.

4. Discussion and Conclusion

In our electron trap system plasma waves can be detected at axial locations of 9 positions during the compression of electrons. In addition to the energy analysis the observation of plasma waves with a spatial resolution may be the advantage in the investigation on space-charge effects of electron beam. However, it is necessary to identify the relationship of parameters between the electron plasma and electron-beam system [1].

In conclusion, we studied on compression of the density distribution of a pure electron plasma confined in a Malmberg-Penning Trap in Kanazawa University. On-axis density increases for 6.8 times higher than that of initial state under application of an external rotating electric field that couples to Trivelpiece-Gould modes. Axial compression of the density distribution for a factor of two is achieved by controlling the confined potential at both ends of the plasma. Substantial increase of the axial kinetic energy was observed during the axial compression.

References

[1] H. Okamoto, H. Tanaka, "Proposed experiments for the study of beam halo formation", *Phys. Res.* A **437** pp178-187 (1999).

[2] E. M. Hollmann, F. Anderegg, and C.F. Driscoll, "Confinement and manipulation of non-neutral plasmas", *Phys. Plasmas.* **7** pp.2776 (2000).

[3] J. R. Danielson and C.M. Surko, "Torque –Balanced High-Density Steady States of Single –Component Plasmas", *Phys. Rev. Lett.* **94** 035001 (2005).

[4] J. H. Malmberg and J. S. deGrassie, "Properties of a Nonneutral Plasma", *Phys. Rev. Lett.* **35**, 577 (1975).

[5] Y. Kiwamoto, K. Ito, et al, "Dynamics of Electron –Plasma Vortex in Background Vorticity Distribution", *Phys. Rev. Lett.* **85** pp3173 - 3176 (2000).

[6] D. L. Eggleston, C. F. Driscoll, et al. "Parallel energy analyzer for pure electron plasma devices" *Phys. Fluids. B* **4** pp.3432-3439 (1992).

[7] Y. Soga, T. Mimura, et al, "Mechanisms of E × B Drift Rotation of a Vortex String in a Pure Electron Plasma", *Plasmas. Fusion. Res.* **8** 2401034 (2013).